To be submitted to
Nucl. Instr. & Meth.

ISTITUTO NAZIONALE DI FISICA NUCLEARE
Laboratori Nazionali di Frascati

LNF-82/80(P)
10 Novembre 1982

M. Anghinolfi, G.P. Capitani, P. Corvisiero, E. De Sanctis, P. Di Giacomo, C. Guaraldo, V. Lucherini, E. Polli, A.R. Reolon, G. Ricco, M. Sanzone, R. Scrimaglio and A. Zucchiatti: THE LEALE PHOTON BEAM FACILITY AT FRASCATI, OBTAINED BY POSITRON ANNIHILATION ON A LIQUID HYDROGEN TARGET.

Servizio Documentazione
dei Laboratori Nazionali di Frascati

INFN - Istituto Nazionale di Fisica Nucleare
Servizio Documentazione

LNF-82/80(P)
10 Novembre 1982

THE LEALE PHOTON BEAM FACILITY AT FRASCATI, OBTAINED BY POSITRON ANNIHILATION ON A LIQUID HYDROGEN TARGET

G.P. Capitani, E. De Sanctis, C. Guaraldo, P. Di Giacomo, V. Lucherini, E. Polli, A.R. Reolon and R. Scrimaglio
INFN - Laboratori Nazionali di Frascati, C.P. 13 - 00044 Frascati (Italy)

M. Anghinolfi, P. Corvisiero, G. Ricco, M. Sanzone and A. Zucchiatti
Istituto di Scienze Fisiche dell'Università di Genova and INFN - Sezione di Genova, V.le Benedetto XV, 5 - 16132 Genova (Italy)

ABSTRACT

The Frascati positron beam is used to produce a quasi-monochromatic annihilation photon beam with a continuously variable energy in the 100-300 MeV range. The positron production, beam transport and monitor system are discussed. The photon facility, with liquid hydrogen target, on-line pair spectrometer and monitor systems, is described. The performance of the facility is shown by the first measurements of Bi photofission and deuteron photodisintegration.

1. - INTRODUCTION

One difficulty in the investigation of photonuclear reactions with real photons is the lack of suitable powerful gamma sources of variable energy. In flight positron annihilation has been widely used in recent years to obtain quasi-monochromatic photon beams[1]. However, because of the necessary double conversion (electrons to positrons and positrons to photons), high current electron accelerators are needed with this technique.

In this paper we describe the LEALE (Laboratorio Esperienze Acceleratore Lineare Elettroni) monochromatic gamma beam facility from the Frascati linac positron beam[2]. Section 2. describes the positron production and acceleration system in the Frascati linear accelerator. Section 3. reports the main features of the positron beam handling system and of the positron beam at the annihilation target. Section 4. describes in detail the characteristic of the monochromatic gamma beam produced by positron annihilation on hydrogen. Section 5. gives the first results of Bismut photofission and deuteron photodisintegration measurements.

2. - POSITRON PRODUCTION AND ACCELERATION

The Frascati linear accelerator[3] is made up of twelve sections: four low energy guides, capable of accelerating a 420 mA electron beam to 65 MeV, and eight high energy guides capable of accelerating, together with the low energy guides, a 100 mA electron beam to 375 MeV. RF power is supplied to the guides by six S-band Thomson-Varian klystrons, each pulsed by a modulator (4 μsec pulse length, 200 pulses per second maximum rate).

Positrons are generated in a high Z conversion target by bremsstrahlung production and subsequent pair production from the high current-low energy electron beam, at the end of the first four sections of the linac. The system for positron production and acceleration includes:

a) a new design electron to positron conversion target (in operation since June 1980), consisting of a disk-shaped gold dowel (1 radiation lenght thick, diameter 5 mm), cast inside a water-cooled copper disk frame[4] (see Fig. 1). This converter can be inserted into the electron beam without disrupting the accelerator vacuum. The electron beam is focused on the target on a circular spot of 1.0 mm diameter, and the target can be moved by remote control (setting accuracy $\pm$0.2 mm) so that the beam can strike different position on the surface;

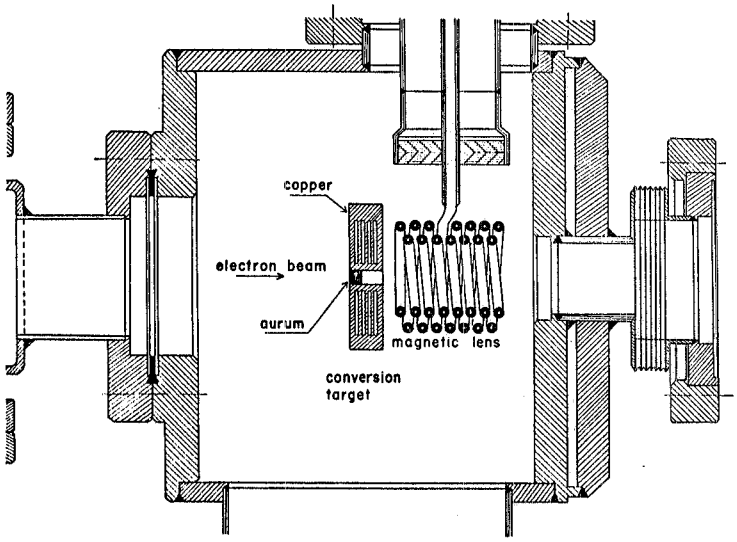

FIG. 1 - Cross section of positron converter region showing the target and the magnetic lens.

b) a new design magnetic lens used to match the emittance of the outgoing positron (small dimensions and large divergence) to the acceptance of the linac (large dimensions and small divergence). The lens (in operation since June 1980) consists of a short copper solenoid (15 turns, 4.5 cm length) set 0.5 cm away from the conversion target. Its axial magnetic field is bell-shaped, with a maximum value of 1.777 T[5];

c) the eight high energy sections, which can accelerate positrons up to 310 MeV. Each section is equipped with a full length (5 m) solenoid producing a uniform static axial magnetic field of 0.24 T. The problem of solenoid misalignment with respect to the axis of the section was solved by mounting soft iron plates at the beginning and end of each section. The plates, centered on the linac axis, affect the fringing field configuration centering it with respect to the beam. The transverse magnetic field component, due to the solenoid tilting with respect to the section centerline, is compensated using two steering fields per section.

3. - THE POSITRON BEAM

3.1. - Positron Beam Transport

An overall view of the LEALE photon facility is given in Fig. 2. The first part of the positron beam handling system, from the end of the linac up to the deviation system, is the same as that used to transport the electrons to produce a secondary pion beam[6]. It consists of three quadrupole doublets (Q_1-Q_2, Q_3-Q_4 and Q_5-Q_6) and four collimators (C_1÷C_4: 25 mm, 25 mm, 25 mm and 40 mm diameter, respectively). Due to the large positron beam emittance (πx10 mm x mrd) the quadrupole polarities and strengths have been calculated to provide a beam with quite constant shape, so as to ensure greater stability and improve transmission through the beam channel[7].

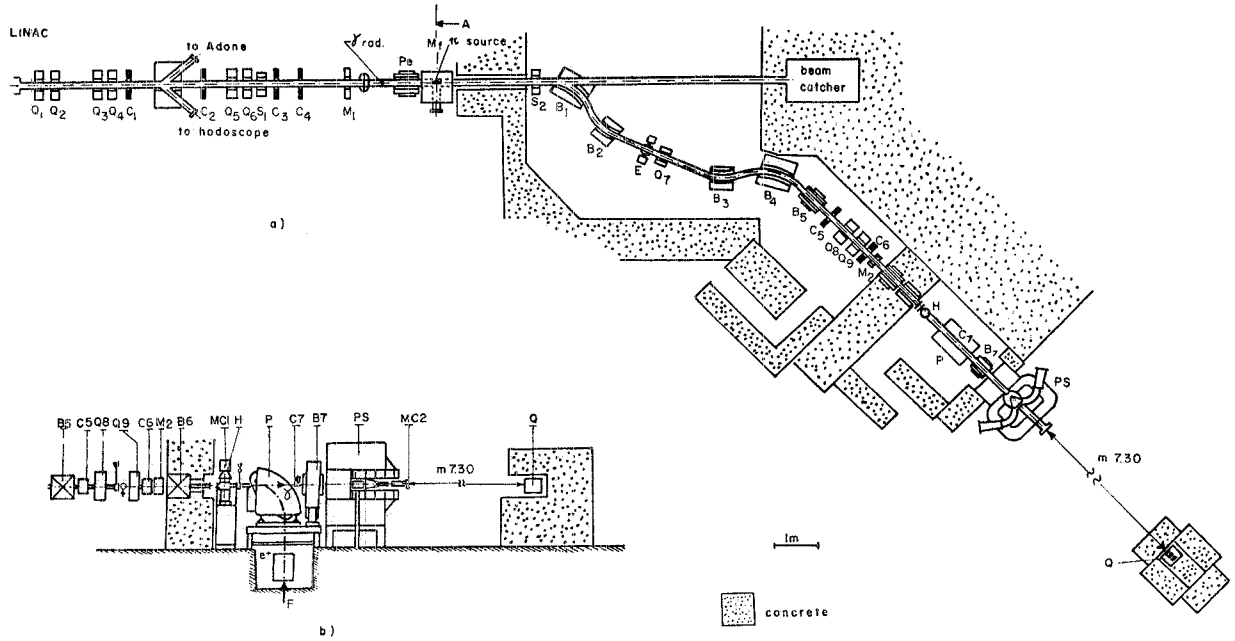

FIG. 2 - Experimental layout of the LEALE photon beam facility: (a) top view, (b) size view of the end section. Q_1÷Q_9 quadrupole magnets, B_1÷B_7 dipole magnets, C_1÷C_7 collimators, E energy slits, F Faraday cup, H hydrogen target, M_1-M_2 ferrite monitors, MC1-MC2 beam profile monitors, P sweeping magnet, PS pair spectrometer, Q quantameter, S_1-S_2 steering coils.

The pulsed magnet inserted after collimator C_1 allows the beam to be deflected into the ADONE storage ring, or transmitted into the LEALE area, or energy analysed. For the latter operation, one beam pulse per second is deflected into an analysing magnet which has in its focal plane a detector system of secondary emission monitors (hodoscope) that provides on-line measurement of the beam energy spectrum.

The second beam handling stage is costituted by a 45° deflection achromatic system, consisting of four magnets (B_1÷B_4) with uniform fields and non-zero entrance and exit angles, to provide double focusing on the annihilation target[8]. The deflection angles are respectively $\vartheta_{B_1}=\vartheta_{B_4}=60°$ and $\vartheta_{B_2}=\vartheta_{B_3}=37.5°$.

Beam energy selection is provided by two tantalum slits, E, 15 mm thick, in the symmetry plane of the achromatic system. The energy calibration of the slits was performed by comparison with the positron energy spectrum measured by the hodoscope.

Three pairs of steering coils along the line enable the positron beam to be centered on the annihilation target. The size and position of the beam on the target are controlled by a beam profile monitor, MC1, consisting

of a bi-gap multiwire chamber, which permits both vertical and horizontal beam profiles to be displayed on an oscilloscope screen[9]. The beam spot is elliptical, with radial and vertical semiaxes measuring 6 mm and 4 mm respectively. Fig. 3 shows a typical beam profile display.

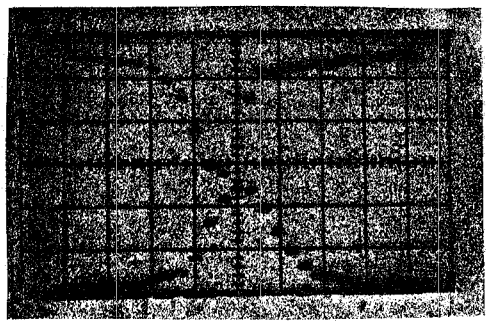

FIG. 3 - Vertical (up) and horizontal (down) positron beam profiles, as seen on the oscilloscope (wire spacing 2 mm), measured at the annihilation target position. Positron energy 180 MeV, peak current 50 μA; chamber high voltage 1500 V.

A precise definition of the photon emission angle is obtained only through a very accurate alignment of the positron beam along the optical axis of the channel. It is possible to achieve this by optimizing the positron current transmitted through two removable copper collimators (C_5 and C_6, diameters respectively 7 mm and 6 mm, thickness 4.0 cm each and placed $\sim$ 4.0 m and $\sim$ 1.75 m before the annihilation target) by means of different sets of steering coils. The focusing quadrupole doublet, Q_7 and Q_8, which is generally turned off, is also used to test whether alignment is correct by checking the absence of steering effects due to the quadrupole fields on the beam profile monitor.

The positron incidence angle on the target may be adjusted between 0° and 1.5° by two dipole magnets (B_5 and B_6 in Fig. 2), giving two vertical deflections of opposite sign, monitored by the positron beam profile chamber. In such a way it is possible to improve the annihilation to bremsstrahlung photon ratio[10].

3.2. - Positron Beam Features

The intensity of the positron beam is continuously monitored at two points of the transport channel, M1 and M2 in Fig. 2, by non-intercepting current trasformers, each consisting of a ferrite toroid. The positron beam acts as the primary of the transformer, while the secondary is a 20-turn coil wrapper around the toroid. The signal feeds a low impedence preamplifier-integrator, placed near to the monitor. The preamplifier-integrator output signal is again amplified, and sent to the control room. The signal to noise ratio is $\sim$ 10 for signals of some mV amplitude at the amplifier-integrator output. A calibration test pulse induced by a standard current is sent, through a one-loop coil wrapped around the ferrite toroid, $\sim$15 μs after the beam pulse, the beam and test signals being simultaneously displaced on an oscilloscope.

The absolute value of the positron current on the target is measured by a Faraday cup (also used as a beam catcher), placed in the focal plane of a damping magnet behind the annihilation target. This magnet sweeps off from the photon beam the positrons that have not undergone annihilation. The Faraday cup has a central core consisting of a cylindrycal lead beam stopper, 30 cm diameter, total thickness 15 cm, which can absorb positrons up to 400 MeV. The core is mounted inside a static vacuum envelope closed by a thin ($\sim$ 2 mm) entrance window. The current is sent directly to a standard current integrator and digitizer (ORTEC Mod. 439).

Fig. 4 gives the average positron current measured with the Faraday cup in the 100÷300 MeV range. The individual points, obtained during different experimental runs, fluctuate according to the machine and conversion target conditions (mean life of the converter $\sim 350 \times 10^6$ pulse), but span the area between the dashed curves. The continuous line connects the central points of the region.

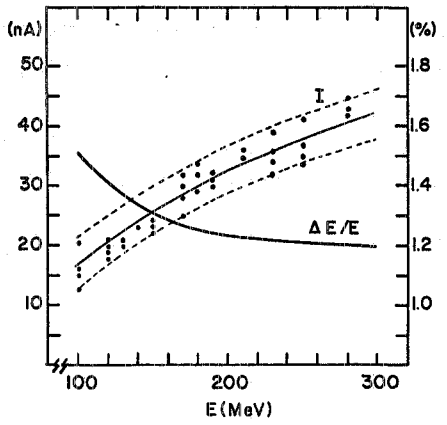

FIG. 4 - Measured positron current, I (right scale), and energy resolution $\Delta E/E$ (left scale) as a function of positron energy E.

Fig. 4 also gives the positron energy resolution, determined by measuring the charge collected by the Farady cup with the energy selection slits E in different positions.

4. - THE PHOTON BEAM

4.1. - Hydrogen Target

Positrons leave the beam pipe through an aluminium window (0.05 mm thick) and annihilate on a liquid hydrogen target (0.0118 radiation lengths thick). The hydrogen cell is a kapton cylinder, 105 mm long, with a diameter of 55 mm (wall thickness 0.125 mm). The cell is contained in a vacuum steel tank, with a thin kapton beam entrance window, 0.12 mm thick. A hydrogen target has been preferred chiefly on account of the reduced intensity of the bremsstrahlung tail of the photon spectrum thus obtained (the ratio of annihilation to bremsstrahlung yields scales as $(Z+1)^{-1}$), in spite of the need to use windows and a kapton cell.

The hydrogen cell can be removed from the beam path remotely, allowing the insertion of the beam profile monitor or of a gold target (0.0118 radiation lengths thick) for the production of a quasi-pure bremsstrahlung photon beam.

The hydrogen target is equipped with a two stages local refrigerator (Cryodine helium refrigerator Mod. 360), installed directly on the hydrogen cell, which makes it possible to liquify only the required quantity of hydrogen. The system (see Fig. 5) consists of a hydrogen gas reservoir, a helium compressor, an absorption trap and a refrigerator.

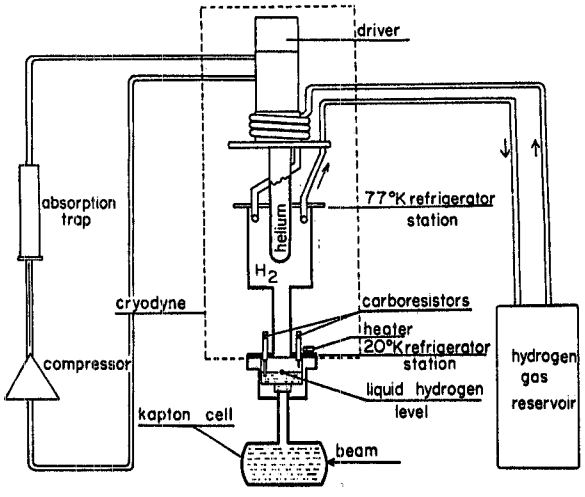

FIG. 5 - Hydrogen target system.

The hydrogen gas leaves the tank at room temperature and at a pressure of 1.6 atm, then passes through two stages of a refrigerator (with a load capacity of 5÷7 Watts at 20°K) where it is chilled and condenses, filling the cell.

A series of thermoresistors placed in the cell and inside the refrigerator monitor the level of liquid hydrogen and ensure the automatic operation of the entire system. The time required to fill the cell with liquid hydrogen is about 3 hours.

By monitoring continuously the hydrogen vapor pressure we are able to keep the liquid hydrogen density constant within 1%[11].

4.2. - Pair Spectrometer

The photon beam is defined by five cylindrical lead collimators (diameters respectively 9.0 mm, 10.0 mm, 10.5 mm, 11.5 mm and 12.2 mm; length 10.0 cm each), inserted in the yoke of the dumping magnet P. The next dipole magnet B7 sweeps the beam of charged background particles produced in the collimators.

A rectangular flat pole (size 40 x 90 cm^2, gap 15 cm) C-type magnet is used as an on-line pair spectrometer[12]. Photons enter the magnetic field region through a hole (diameter 4 cm), opened in the yoke of the magnet and are converted by one of the five available, remotely selectable, aluminium targets. Each target is thin enough ($\lesssim 5\times10^{-4}$ radiation lengths) to make negligible both beam attenuation and loss of efficiency due to multiple scattering and energy loss. In order to reduce background production from air, the beam channel is vacuumized from the hydrogen target up to the spectrometer exit window (Kapton sheet 0.123 mm thick).

Electrons and positrons, after $\sim 110°$ deflection by the spectrometer magnet, leave the vacuum chamber by passing through an aluminium window 1 mm thick, and are detected by two identical arrays of four counters (E_1,.., E_4 and P_1,.., P_4; dimensions: 1 x 2 x 10 cm^3 each) set along the focal line, followed by a fifth backing counter (E_5, P_5).

For each setting of the magnetic field the spectrometer defines sixteen energy channels which can be grouped into seven independent energy bins. The $E_i(P_i)$ discriminator outputs are sent to an OR circuit and then to a double coincidence with the $E_5(P_5)$ counter. A good event is defined by coincident signals from the two arms. Real and accidental coincidence signals enable the acquisition, via CAMAC, on a PDP 15/76 computer of the signals from the E_i and P_i counters. The computer processes on line the events and displays the photon energy spectrum alive on a storage display scope.

Details on the optical properties of the magnet, calculation of the response function, by means of a Monte Carlo code, and spectrometer performances are given in Ref. (12). Fig. 6 shows the calculated resolution ε and

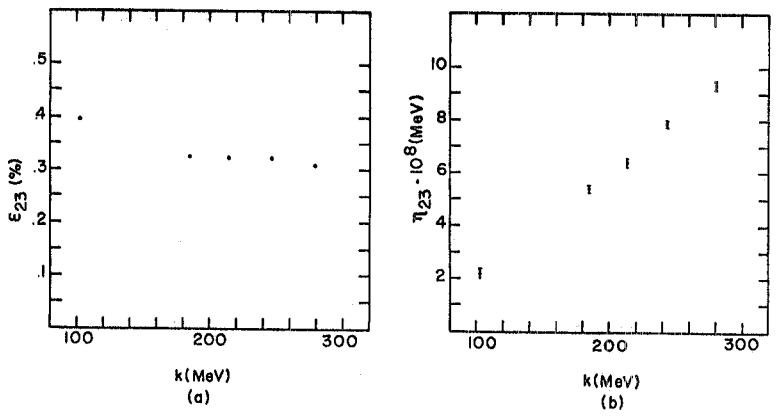

FIG. 6 - Calculated values of relative resolution ε_{23}(FWHM) (a) and efficiency η_{23} (b) of the E_2P_3 counter couple of the pair spectrometer as a function of the photon energy k.

efficiency η (defined as the probability of pair production and detection) of the E_2 P_3 counter couple, as a function of the photon energy k. Similar values have been obtained for all counter couples, $E_i P_j$.

4.3. - Photon Beam Features

The total energy of the photon beam is finally measured by a Wilson quantameter, the integration system of which has been modified as suggested in Ref. (13) so as to provide constant sensitivity in our energy range.

The spatial distribution of the photon beam can be measured with a beam profile monitor[9] which can be inserted on the channel just after the pair spectrometer. Fig. 7 shows typical measured photon profiles.

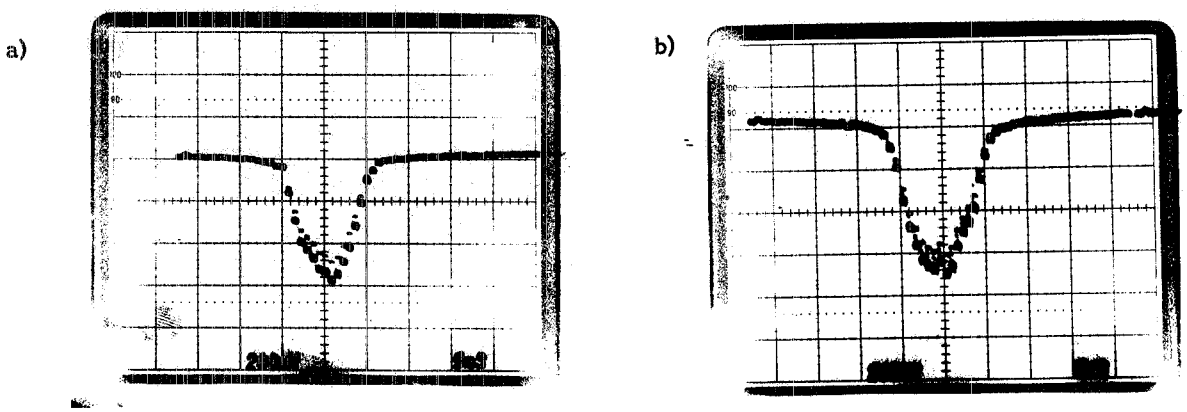

FIG. 7 - Vertical (a) and horizontal (b) photon beam profiles, as seen on the oscilloscope (wire spacing 2 mm), measured at the exit window of the pair spectrometer vacuum chamber. Positron energy 150 MeV, peak current 35 μA; chamber high voltage 4000 V.

Fig. 8 shows six typical energy spectra, measured at different positron energies E and photon collection angles θ_γ. The full line curves have been obtained by a Monte Carlo simulation[14] which takes into account:

a) the positron beam characteristic (energy spread, emittance and incidence angle on the annihilation target);

b) the different processes (annihilation, bremsstrahlung, multiple scattering and energy loss) undergone by positrons in all the materials (hydrogen target, aluminium and mylar windows, air) encountered along the beam path;

c) photon collection characteristics (diameter, thickness and relative position of the collimators).

Computer programmes for the evaluation of photon energy spectra from both positron annihilation and bremsstrahlung have been developed in many laboratories (see references (3) and (4) in Ref. (14)), but none has properly included all the above effects. Our Monte Carlo code calculates correctly both the emittance and the energy spectrum of the quasi-monochromatic photon beam, and gives the absolute value of the photon flux per incident positron. The excellent agreement in Fig. 8 between the computed and measured spectra is obtained by slightly adjusting the values of only two input quantities (positron emittance and photon collection angle) in the Monte Carlo calculation by amounts comprised within the experimental errors.

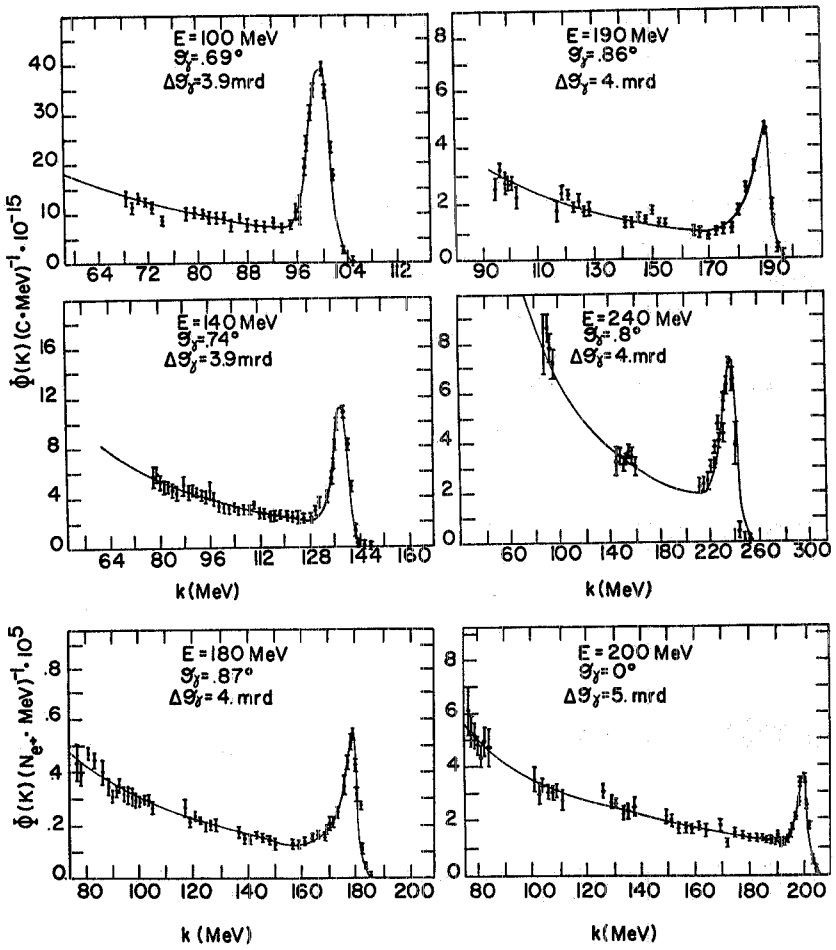

FIG. 8 - Photon energy spectra measured with the pair spectrometer at the given positron energies E, photon collection angle θ_γ and half angular geometric photon acceptance $\Delta\theta_\gamma$. The full lines spectra are calculated with a Monte Carlo program.

To normalize the experimental spectrum to the calculated spectrum, a constant factor is used to take the efficiency of the pair spectrometer into account. The comparison between the calculated and measured values of the beam features has been carried out at many positron energies and in widely different experimental conditions. The agreement has always proved to be excellent by using in any case the same normalization factor. There is therefore evidence that the Monte Carlo results can be assumed to be reliable in all the experimental conditions.

Figs. 9, 10 and 11 give the photon beam characteristics as evaluated by the Monte Carlo calculation. In Fig. 9 the number of annihilation photon per incident positron, N_A/N_{e^+}, and the ratio between annihilation and bremsstrahlung photons, N_A/N_B, are plotted as a function of positron energy E and for set values of the photon collection angle θ_γ (N_B is the total number of bremsstrahlung photons in the spectrum with energy greater than 10 MeV).

It can be seen from the figure that the annihilation yield for photon emission angles $\theta_\gamma = 0° \div 0.5°$ increases with E, while at the same time the yield of unwanted bremsstrahlung photons increases even faster with increasing E, so that the bremsstrahlung contribution progressively submerges the annihilation peak. The situation changes drastically for all $\theta_\gamma > 0.5°$: the annihilation intensity decreases with E, but the bremsstrahlung

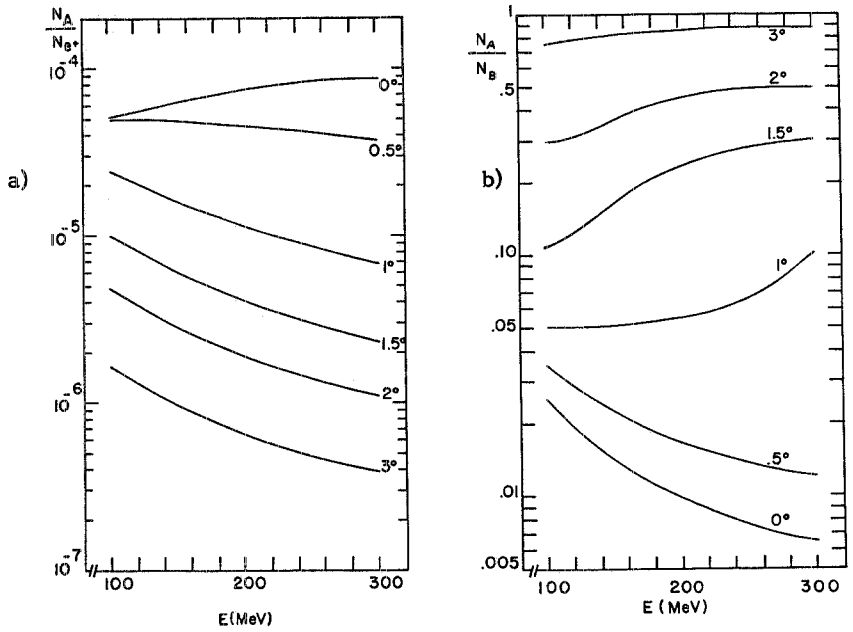

FIG. 9 - Properties of the annihilation photon beam as obtained from a Monte Carlo calculation. Figure (a) gives the number of monochromatic photons per positron, N_A/N_{e^+}, and (b) the ratio of annihilation to bremsstrahlung photons, N_A/N_B, as a function of the positron energy E for a few values of the photon collection angle. Input data for the calculation: positron energy spread: 1.58%; positron emittance: radial 18 mm x mrd, vertical 15 mm x mrd; annihilation target: liquid hydrogen 0.0118 radiation lengths thick; geometric solid angle of photon collection: 5.10^{-5} sr.

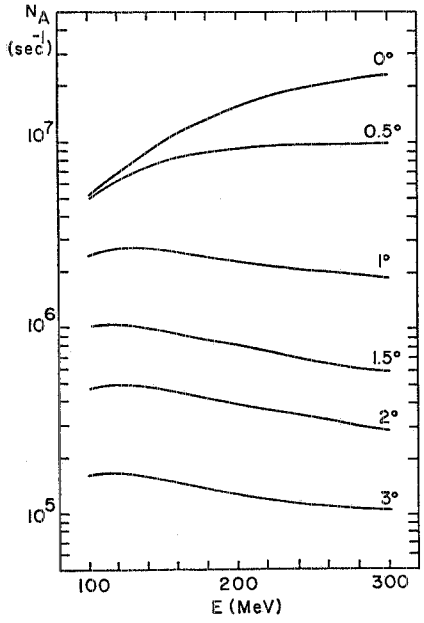

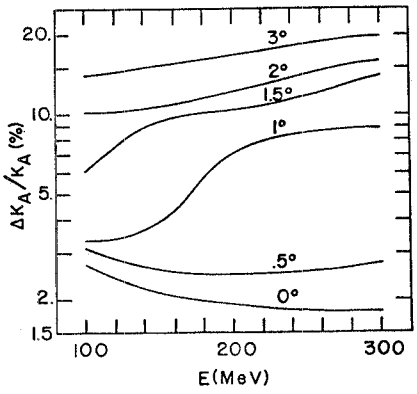

FIG. 10 - Evaluated resolution $\Delta k_A/k_A$ (FWHM) of the annihilation photon peak as a function of positron energy E and photon collection angle (same conditions as in Fig. 9).

FIG. 11 - Number of annihilation photons per second as a function of the positron energy E and of the photon collection angle θ_γ. Same conditions as in Fig. 9. Assumed positron current corresponds to the solid line in Fig. 4.

intensity decreases with increasing E and θ_γ much more rapidly than that of the annihilation radiation. It is therefore possible to increase the N_A/N_B ratio at the expense of intensity and peak resolution by collecting photons at the largest possible angles.

Fig. 10 gives the evaluated resolution of the annihilation peak $\Delta k_A/k_A$ (FWHM), as a function of the positron energy and for various θ_γ.

In Figs. 9 and 10 the above change in the behaviour of the quantities in the ordinates is more evident in the region $0.5° \lesssim \theta_\gamma \lesssim 1.0°$. This is due to the multiple scattering effects in the annihilation target, which spread the positron trajectories inside an angular cone whose aperture, especially at lower energies, is comparable with the chosen photon collection acceptance ($\sim \pm 4$ mrd), and to the positron beam cross section area, which is also comparable with the collimator holes.

Finally, Fig. 11 gives the calculated intensity of the annihilation peak, as a function of E and for various θ_γ. The curves have been obtained by using the average values of the positron current given by the solid line in Fig. 4.

5. - SAMPLE DATA FROM EXPERIMENTS

To date the LEALE photon beam has been used in two experiments:

1 - photofission of bismut,

2 - deuteron photodisintegration.

In the first experiment a metal target of natural Bi (with surface area of 50x50 mm^2 and thickness of 0.1 mm) was set at the output window of the pair spectrometer vacuum chamber. The target was sandwiched between two plates of glass which covered all the sample. The fission fragments were detected by means of the glass sandwiches technique described in ref. (15). The yields were obtained by counting the number of fission tracks in the scanned surface and measuring the exposure dose with the quantameter. The exposures were taken at 16 positron energies, ranging from 120 MeV up to 280 MeV, and collecting the photon beam at angles $0.5° \lesssim \theta_\gamma \lesssim 1°$. The photofission cross section σ_f is related to the experimental yields $y(k_A)$ by the following integral equation:

$$y(k_A) = \int_{k_T}^{k_M} \Phi(k, k_A)\, \sigma_f(k)\, dk,$$

where k_T is the energy of the photofission threshold, k_M is the maximum photon energy and $\Phi(k, k_A)$ is the photon beam spectrum as a function of the gamma energy k and of the annihilation peak energy k_A. The advantage of using the LEALE quasi-monochromatic photon beam in order to perform photofission measurements is analyzed in ref. (16). The preliminary results of the bismut photofission cross section have been published elsewhere[17]. Here we show in Fig. 12 the experimental yields as a function of k_A.

In the deuteron photodisintegration[18] the used target was a vertical mylar cylindrer (4.0 cm diameter, wall thickness 0.08 mm) filled up with liquid deuterium. The ejected photons were detected by five E, dE/dx spectrometer mounted on arms which can be rotated around the target. Each spectrometer consisted of a thin (3 mm) plastic scintillator and a cylindrical NaI crystal (11 cm diameter by 5 cm thick) having a 2.5% FWHM intrinsic resolution[19]. Data were recorded and on-line processed on a PDP 15/76 computer. The proton angular distribution has been measured at 7 positron energies, ranging from 100 MeV up to 250 MeV and collecting the photon beam at $\theta_\gamma \sim 0.75°$ by respect to the positron beam flight direction.

The results of this experiment will be published elsewhere. However, we show in Fig. 13 typical proton

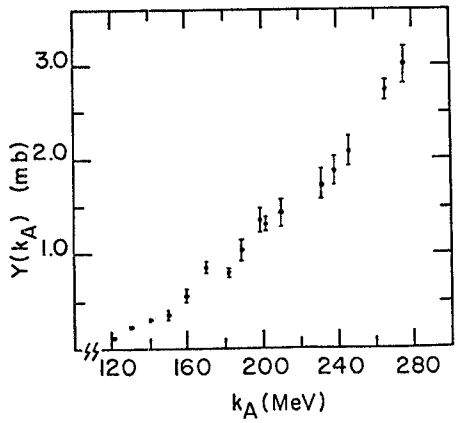

FIG. 12 - Photofission yields per equivalent quantum of Bi as a function of the annihilation peak energy k_A.

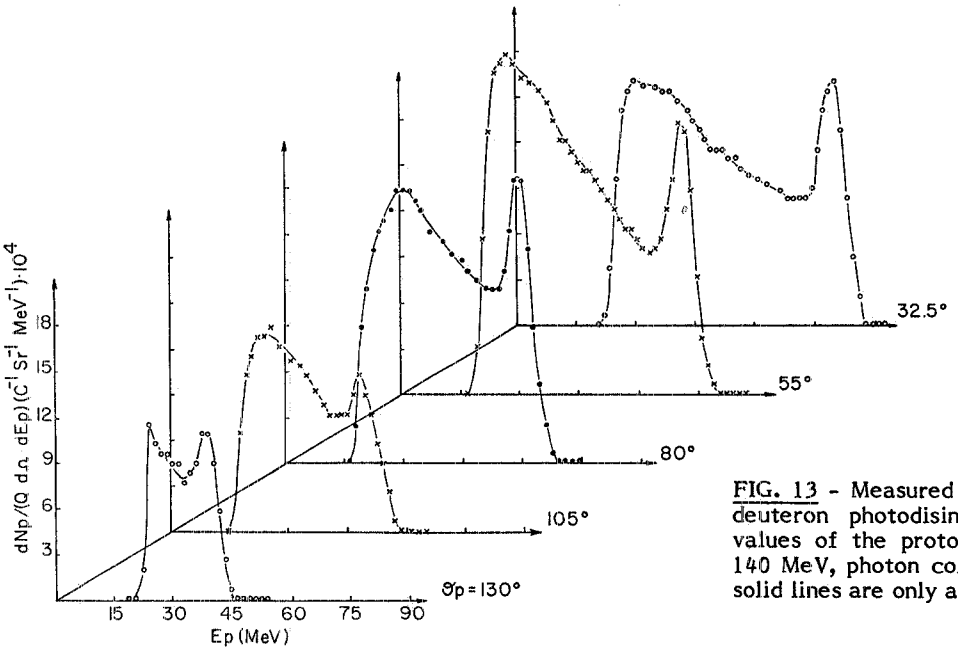

FIG. 13 - Measured proton energy spectra from deuteron photodisintegration, for the settled values of the proton angle θ_p. Positron energy 140 MeV, photon collection angle θ_γ=0.75°. The solid lines are only a guide for the eye.

energy spectra induced by a 140 MeV annihilation photon beam, for the 5 settled values of the proton angle θ_p.

6. - SUMMARY

The performance of the LEALE facility at the Frascati linear accelerator has been described. Intensity and energy resolution of nearly monoenergetic annihilation photons have been measured, from which the linac and facility requirements for undertaking photonuclear experiments may be derived. The first series of experiments have shown that this photon beam is a suitable tool for the investigation of photonuclear processes in the photon energy range 100÷300 MeV.

ACKNOWLEDGEMENTS

The construction and testing of the LEALE photon beam involved many people whose contributions were of notable importance. While we regret not to be able to singly thank all of them, we would remember the great help received from the Machine and Technical Departments of the Frascati Laboratories, which provided efficient improvements and maintenance of the linac. Particular thanks are also due to the technical staffs of the LEALE and Genova groups for their continuous assistance.

REFERENCES

(1) R. Leicht, K.P. Schelhaas, M. Hammen, J. Ahrens and B. Ziegler, Nuclear Instr. & Meth. 179, 131 (1981); A. Veyssiere, H. Beil, R. Bergère, P. Carlos, J. Fagot, A. Leprêtre anf J. Ahrens, Nuclear Instr. & Meth. 165, 417 (1979); E. Hayward, W.R. Dodge and B.H. Patrik, Nuclear Instr. & Meth. 159, 289 (1979); U. Kneissl, E.A Koop, G. Kuhl, K.H. Leister and A. Weller, Nuclear Instr. & Meth. 127, 1 (1975); D. Blum, J. Bouchort, B. Grossetête, W. Mc Gill and A. Nguyen Ngoc, Nuclear Instr. & Meth. 115, 553 (1974); S.C. Fultz, R.L. Bramblett, J.T. Caldwell and N.A. Ken, Phys. Rev. 127, 1293 (1962).

(2) G.P. Capitani, E. De Sanctis, P. Di Giacomo, C. Guaraldo, G. Ricco, M. Sanzone, R. Scrimaglio and A. Zucchiatti, Proc. Few Body Systems and Electromagnetic Interactions, Ed. by C. Ciofi degli Atti and E. De Sanctis, Lectures Notes in Physics (Springer Verlag, Berlin 1977), vol. 86 pag. 127; Frascati Report LNF-77/45 (1977).

(3) Varian Associates Technical Report R 63, April 24 (1963); F. Amman and A. Andreani: Frascati Report LNF-63/46 (1963); C. Nunan, IEEE Trans. on Nuclear Sci. NS-12, 465 (1965); F. Amman, R. Andreani, J. Haimson and C. Nunan, Frascati Report LNF-66/69 (1966).

(4) A. Cattoni and V. Chimenti, private communication

(5) R. Boni, S. Guiducci and M. Vescovi, Frascati Report LNF-81/6 (1981).

(6) R. Barbini, S. Faini, C. Guaraldo, C. Schaerf and R. Scrimaglio, Nuclear Instr. & Meth. 115, 85 (1974).

(7) G.P. Capitani, E. De Sanctis, S. Faini, C. Guaraldo, R. Malvano, G. Ricco, M. Sanzone and R. Scrimaglio, Frascati Report LNF-72/99 (1972).

(8) E. Mancini and M. Sanzone, Nuclear Instr. & Meth. 66, 87 (1968).

(9) M. Albicocco, G.P. Capitani, E. De Sanctis, P. Di Giacomo, C. Guaraldo, V. Lucherini, E. Polli and A.R. Reolon, Nuclear Instr. & Meth., 203, 63 (1982).

(10) P. Di Giacomo, and V. Lucherini, Frascati Report LNF-78/8 (1978).

(11) M. Albicocco and A. Viticchiè, LEALE internal memorandum unpublished.

(12) G.P. Capitani, E. De Sanctis, P. Di Giacomo, G. Guaraldo, S. Gentile, V. Lucherini, E. Polli, A.R. Reolon and R. Scrimaglio, Nuclear Instr. & Meth. 178, 61 (1980); G.P. Capitani, E. De Sanctis, S.Pasquini and A.R. Reolon, Frascati Report LNF-78/2 (1978); S. Pasquini and A.R. Reolon, Frascati Report LNF-77/34 (1977).

(13) A.P. Komar, S.P. Kruglov and I.V. Lopatin, Nuclear Instr. & Meth. 82, 125 (1970).

(14) G.P. Capitani, E. De Sanctis, P. Di Giacomo, C. Guaraldo, V. Lucherini, E. Polli, A.R. Reolon and V. Bellini, Nuclear Instr. & Meth. 203, 353 (1982).

(15) G. Bologna, V. Bellini, V. Emma, A.S. Figuera, S. Lo Nigro, C. Milone and G.S. Pappalardo, Nuovo Cimento 35A, 91 (1976) and 47A, 529 (1978).

(16) E. De Sanctis, P. Di Giacomo, S. Gentile, V. Lucherini, E. Polli, A.R. Reolon, V. Bellini, S. Lo Nigro and G.S. Pappalardo, Nuclear Instr. & Meth. 203, 227 (1982).

(17) V. Bellini, E. De Sanctis, P. Di Giacomo, V. Emma, C. Guaraldo, S. Lo Nigro, V. Lucherini, C. Milone, G.S. Pappalardo, E. Polli and A.R. Reolon, Frascati Report LNF-82/60(P) and Lett. Nuovo Cimento in press.

(18) G.P. Capitani, E. De Sanctis, P. Di Giacomo, C. Guaraldo, G. Ricco, M. Sanzone, R. Scrimaglio and A. Zucchiatti, Frascati Report LNF-77/35 (1977).

(19) A. Zucchiati, M. Sanzone and E. Durante, Nuclear Instr. & Meth. 129, 467 (1975).